Langmuir−Blodgett Films of Known Layered Solids: Preparation and Structural Properties of Octadecylphosphonate Bilayers with Divalent Metals and Characterization of a Magnetic Langmuir−Blodgett Film

Candace T. Seip,[†] Garrett E. Granroth,[§] Mark W. Meisel,*[,§] and Daniel R. Talham*[,†]

Contribution from the Department of Chemistry, University of Florida, Gainesville, Florida 32611-7200, and Department of Physics and Center for Ultralow Temperature Research, University of Florida, Gainesville, Florida 32611-8440

Received October 15, 1996[⊗]

Abstract: Langmuir−Blodgett (LB) films of a series of divalent metal octadecylphosphonates have been prepared and characterized. The films are each shown to be LB analogs of known solid-state metal phosphonates possessing 2-dimensional ionic−covalent metal phosphonate layers. The metal phosphonate layers crystallize during the LB deposition process. Films were characterized with XPS, X-ray diffraction, ellipsometry, attenuated total reflectance FTIR, and, in the case of the manganese film, SQUID magnetometry. Octadecylphosphonate films with Mn^{2+}, Mg^{2+}, and Cd^{2+} form with the stoichiometry $M(O_3PC_{17}H_{37})\cdot H_2O$ and have metal phosphonate bonding consistent with the analogous $M(O_3PR)\cdot H_2O$ layered solids. The Ca^{2+} film forms as $Ca(HO_3PC_{18}H_{37})_2$, which is also a known solid-state phase. Magnetic measurements reveal that the manganese octadecylphosphonate film undergoes a magnetic ordering transition at 13.5 K resulting in a "weak ferromagnet". The behavior is similar to that of the known layered solid-state manganese alkylphosphonates which are also "weak ferromagnets". The magnetic ordering is antiferromagnetic where incomplete cancellation of the magnetic sublattices, due to low site symmetry, results in a spontaneous magnetization. A spin-flop transition is observed at 2.5 T in magnetization *vs* applied field measurements of the ordered state. The film also exhibits magnetic memory, with a small remnant magnetization and a coercive field of 20 mT at 2 K. The results demonstrate that magnetic ordering phenomena can be incorporated into LB films and that LB film methods can be used to prepare monolayer and multilayer films of known solid-state materials.

Introduction

There is currently high interest in engineering mixed organic/inorganic materials where features of the organic and inorganic components complement each other leading to new solid-state structures and materials with composite or even new properties. Some examples of recent interest are layered inorganic solids with organic intercalates,[1,2] organic/inorganic low-dimensional solids,[3−6] zeolites and other open framework host materials with organic guests,[7,8] metal oxide mesostructures formed with the aid of organic surfactants,[9−11] and thin film heterostructures built up from alternating layers of organic polyelectrolytes and colloidal inorganic polyions.[12,13] In some cases, a stable inorganic lattice facilitates spatial and orientational control of organic molecules. On the other hand, new inorganic lattice structures are sometimes formed resulting from cooperative interactions between the organic and inorganic components. In all cases, there is the promise of developing new materials with properties not seen in purely organic or purely inorganic solids.

The Langmuir−Blodgett technique[14−18] is one of the oldest and most elegant approaches known that allows researchers to purposefully arrange molecules into organized assemblies. Molecules, usually amphiphiles, are first compressed to a close-packed monolayer at a water surface followed by transfer of the assembly as a monolayer to a solid support. Multilayer films are formed through repeated deposition cycles. While the LB method is normally considered a technique for organizing organic molecules, inorganic ions are often incorporated into transferred films.[14,16,17] The metal ions cross-link charged molecules and enhance the films' stability and ease of processing, but they are generally thought of as passive elements in

* Authors to whom correspondence should be addressed.
[†] Department of Chemistry.
[§] Department of Physics and Center for Ultralow Temperature Research.
[⊗] Abstract published in *Advance ACS Abstracts,* July 1, 1997.

(1) Bringley, J. F.; Averill, B. A. *Chem. Mater.* **1990**, *2*, 180−186.
(2) Kanatzidis, M. C.; Wu, C.-G.; Marcy, H. O.; Kannewurf, C. R. *J. Am. Chem. Soc.* **1989**, *111*, 4139−4141.
(3) Cao, G.; Hong, H.-G.; Mallouk, T. E. *Acc. Chem. Res.* **1992**, *25*, 420−427.
(4) Day, P. *Phil. Trans. R. Soc. London A* **1985**, *314*, 145−158.
(5) Day, P.; Ledsham, R. D. *Mol. Cryst. Liq. Cryst.* **1982**, *86*, 163−174.
(6) Thompson, M. E. *Chem. Mater.* **1994**, *6*, 1168−1175.
(7) Ozin, G. A. *Adv. Mater.* **1992**, *4*, 612−649.
(8) *Supramolecular Architecture. Synthetic Control in Thin Films and Solids*; Bein, T., Ed.; American Chemical Society: Washington DC, 1992; Vol. 499, p 441.
(9) Beck, J. S.; Vartuli, J. C.; Roth, W. J.; Leonowicz, M. E.; Kresge, C. T.; Schmitt, K. D.; Chu, C. T.-W.; Olson, D. H.; Sheppard, E. W.; McCullen, S. B.; Higgins, J. B.; Schlenker, J. L. *J. Am. Chem. Soc.* **1992**, *114*, 10834−10843.
(10) Monnier, A.; Schuth, F.; Huo, Q.; Kumar, D.; Margolese, D.; Maxwell, R. S.; Stucky, G. D.; Krishnamurty, M.; Petroff, P.; Firouzi, A.; Janicke, M.; Chmelka, B. F. *Science* **1993**, *261*, 1299−1303.
(11) Kresge, C. T.; Leonowicz, M. E.; Roth, W. J.; Vartuli, J. C.; Beck, J. S. *Nature* **1992**, *359*, 710−713.
(12) Keller, S. W.; Kim, H.-N.; Mallouk, T. E. *J. Am. Chem. Soc.* **1994**, *116*, 8817−18.
(13) Kleinfield, E. R.; Ferguson, G. S. *Science*, **1994**, *265*, 370.
(14) Blodgett, K. A.; Langmuir, I. *Phys. Rev.* **1937**, *51*, 964.
(15) Gaines, G. J. *Insoluble Monolayers at Liquid−Gas Interfaces*; Wiley-Interscience: New York, 1966.
(16) *Langmuir−Blodgett Films*; Roberts, G. G., Ed.; Plenum Press: New York, 1990.
(17) Ulman, A. *An Introduction to Ultrathin Organic Films: From Langmuir−Blodgett to Self-Assembly*; Academic Press: Boston, 1991.
(18) Kuhn, H.; Möbius, D.; Bücher, H. In *Physical Methods of Chemistry*; Weissberger, A., Rossiter, B., Eds.; John Wiley and Sons: 1972; Vol. 1, Part IIIB, pp 577−715.

S0002-7863(96)03598-6 CCC: $14.00

the otherwise organic assemblies. While there are recent studies that show how the identity of the inorganic ions can influence the LB film structure,[19] there has been relatively little effort by researchers to control the structure and function of the inorganic component of LB films.[16,17] If the inorganic network can be purposefully developed, then the alternating hydrophobic and hydrophilic layered structure of LB films, coupled with the ability to control layer-by-layer deposition, should provide a unique opportunity to explore the fabrication of mixed organic/inorganic layered solids and thin films.

An approach that we are investigating for controlling the inorganic component of LB films is to base the films on known inorganic layered structures and incorporate an ionic−covalent inorganic lattice into the hydrophilic portion of the LB assemblies.[20−23] There are numerous inorganic and mixed organic/inorganic layered solids,[3−6] and the objective is to use LB methods to prepare examples of these inorganic layers. If the inorganic lattice favors a layered structure it might complement the layered nature of organic LB film assemblies. We have previously demonstrated these concepts[20−22] by characterizing LB films of zirconium octadecylphosphonate and manganese octadecylphosphonate which are each analogs of known metal phosphonate layered solids.[3,24−26] Although the tetravalent and divalent metal phosphonate solid-state structures are slightly different,[3,24−26] these solids are all characterized by sheets of metal ions that are bonded above and below the metal ion plane by layers of the organophosphonates (Figure 1). The phosphonate ligands bridge metal ions forming the inorganic lattice, and adjacent layers are separated by van der Waals interactions between the organic groups. The zirconium phosphonate and manganese phosphonate LB films have been shown to have the same inorganic lattice structure as the analogous solids.[20−22]

This article describes LB films modeled after divalent metal organophosphonates. Thorough structural studies by Mallouk and co-workers[3,26−28] and Cao and co-workers[29] have identified two series of solid-state divalent metal organophosphonates, $M(O_3PR)\cdot H_2O$ (M = Mg, Mn, Zn, Ca, Cd; R = *n*-alkyl, aryl group) and $M(HO_3PR)_2$ (M = Ca). Each forms a layered structure, and interlayer distances vary to accommodate the different R groups. For M = Mg, Mn, and Zn in the first series the layered phosphonates are isostructural, crystallizing in an orthorhombic space group.[26,27] Each phosphonate group bridges four metal ions, and the metal ions are coordinated by five oxygens from four different phosphonate groups. The distorted octahedral coordination of the metal is completed by a water of hydration (Figure 1). For M = Ca or Cd in the same series, a structure of slightly lower symmetry is adopted.[27−29] In the second series, calcium forms 1:2 salts with alkylphosphonates having alkyl chain lengths of five carbon atoms or greater (Figure 1).[27,28]

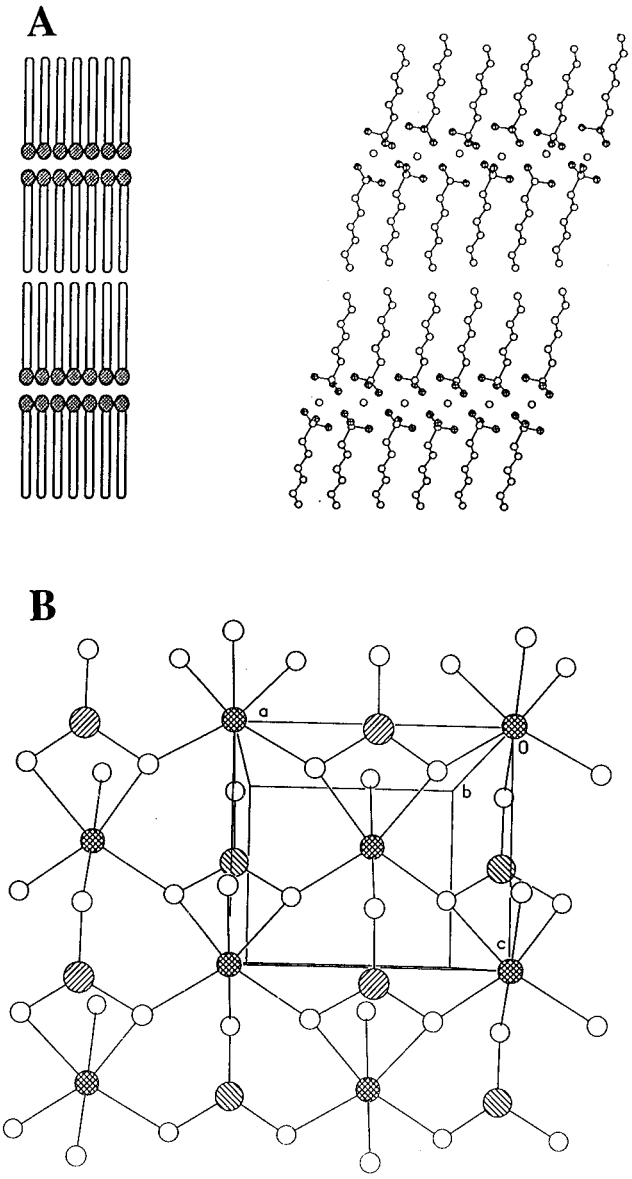

Figure 1. (A) Scheme illustrating the similar layered structures of a Y-type LB film (left) and the layered metal alkylphosphonates, exemplified by $Ca(O_3PC_6H_{12})_2$ (right). The figure at right was generated from crystallographic data taken from ref 28. (B) The manganese ion plane of mangnanese phenylphosphonate viewed perpendicular to the layer. The phenyl groups have been omitted. Each manganese ion is coordinated by five phosphonate oxygens and one water molecule, and each ion is bridged to four nearest neighbors by single phosphonate oxygens. The manganese alkylphosphonates are isostructural with the phenyl analog. Key: oxygen, small open circles; manganese, cross-hatched circles; phosphorus, diagonal-hatched circles (phosphorus atoms above and below the plane are distinguished by hatch marks with different directions). Crystallographic data were taken from ref 26.

In this report, we show how the LB approach for depositing metal phosphonate films is quite general and offer a compelling example of how the choice of metal ion can be used to control the structure of the deposited LB films. We present a detailed description of the preparation and characterization of octadecylphosphonate LB films with a series of divalent metals, including a full account of the preparation of the Mn^{2+} film and new films containing Mg^{2+}, Cd^{2+}, and Ca^{2+}. While different structures are observed, each LB film will be shown to adopt the same metal−phosphonate binding as the known

(19) Zasadzinski, J. A.; Viswanathan, R.; Madsen, L.; Garnaes, J.; Schwartz, D. K. *Science* **1994**, *263*, 1726−1733.
(20) Byrd, H.; Pike, J. K.; Talham, D. R. *Chem. Mater.* **1993**, *5*, 709−715.
(21) Byrd, H.; Pike, J. K.; Talham, D. R. *J. Am. Chem. Soc.* **1994**, *116*, 7903−7904.
(22) Seip, C. T.; Byrd, H.; Talham, D. R. *Inorg. Chem.* **1996**, *35*, 3479−3483.
(23) Byrd, H.; Whipps, S.; Pike, J. K.; Ma, J.; Nagler, S. E.; Talham, D. R. *J. Am. Chem. Soc.* **1994**, *116*, 295−301.
(24) Clearfield, A. *Commenta Inorg. Chem.* **1990**, *10*, 89−128.
(25) Alberti, G.; Casciola, M.; Costantino, U.; Vivani, R. *Adv. Mater.* **1996**, *8*, 291−303.
(26) Cao, G.; Lee, H.; Lynch, V. M.; Mallouk, T. E. *Inorg. Chem.* **1988**, *27*, 2781−2785.
(27) Cao, G.; Lee, H.; Lynch, V. M.; Mallouk, T. E. *Solid State Ionics* **1988**, *26*, 63−69.
(28) Cao, G.; Lynch, V. M.; Swinnea, J. S.; Mallouk, T. E. *Inorg. Chem.* **1990**, *29*, 2112−2117.
(29) Cao, G.; Lynch, V. M.; Yacullo, L. N. *Chem. Mater.* **1993**, *5*, 1000−1006.

solid-state analogs. The Mn^{2+}, Cd^{2+}, and Mg^{2+} octadecylphosphonate LB films form $M(O_3PR)\cdot H_2O$ structures, and the calcium octadecylphosphonate LB film forms with a 1:2 metal:phosphonate stoichiometry and the formula $Ca(HO_3PR)_2$. The different structures demonstrate the important role that the inorganic extended lattice plays in organizing the LB films and that the metal phosphonate LB film structure can be controlled by choice of metal ion.

The addition of a solid-state inorganic lattice into LB films opens the possibility of introducing physical properties that are typical of the inorganic solid-state such as cooperative electronic or magnetic phenomena. As a demonstration of this concept, we report here the characterization of a magnetic LB film. We show that manganese octadecylphosphonate LB films undergo a transition to long-range magnetic order characteristic of a "weak ferromagnet". The manganese phosphonate solids after which the films are modeled are also weak ferromagnets,[30,31] and the ordering temperature in the LB films is nearly the same as those observed for a series of powdered solid-state analogs. The results demonstrate for the first time that LB methods can be used for depositing thin films of known magnetic solids and that magnetic ordering phenomena can be observed in LB films.

Experimental Section

Materials. All chemicals were purchased and used without further purification. Octadecylphosphonic acid, $CH_3(CH_2)_{17}P(O)(OH)_2$, (98%), was purchased from Alfa Aesar (Ward Hill, MA). $MnCl_2\cdot 4H_2O$ (99.6%) and $CaCl_2$ (97.8%) were purchased from Fisher Scientific (Fair Lawn, NJ). $CdCl_2\cdot 2.5H_2O$ was obtained from Aldrich (Milwaukee, Wisconsin). $Mg(NO_3)_2\cdot 6H_2O$ was obtained from Mallinckrodt, Inc. (Paris, KY). Octadecyltrichlorosilane (OTS, $C_{18}H_{37}SiCl_3$, 95%) was purchased from Aldrich and stored under N_2. A Barnstead Nanopure (Boston, MA) purification system produced water with an average resistivity of 18 MΩ cm for all experiments.

Substrate Preparation and Deposition Procedure. Single-crystal (100) silicon wafers, purchased from Semiconductor Processing Company (Boston, MA), were used as deposition substrates for XPS and ellipsometry measurements. Samples for X-ray diffraction were deposited onto glass slides. The silicon and glass substrates were cleaned by using the RCA cleaning procedure[32] then dried under N_2. Germanium attenuated-total-reflectance (ATR) crystals (45° 50 mm × 10 mm × 3 mm), purchased from Wilmad Glass (Buena, NJ), were used as substrates for the infrared experiments. Octadecyltrichlorosilane (OTS) was self-assembled[33,34] onto the substrates to make them hydrophobic. The clean substrates were placed in a 2% solution of OTS in hexadecane for 30 min, rinsed with chloroform to remove any excess hexadecane, and dried under a stream of nitrogen. For magnetic measurements, films were deposited onto Mylar substrates that were primed with 10 LB layers of calcium arachidate.

Divalent metal octadecylphosphonate Langmuir−Blodgett films were prepared by spreading octadecylphosphonic acid onto an aqueous subphase containing a salt of the appropriate metal at a concentration of 5×10^{-4} M. The pH of the subphase was adjusted appropriately with HCl or KOH. Target pressures and subphase pH varied depending on the metal used, as recorded in Table 1.

Instrumentation. The LB films were prepared by using a KSV (Stratford, CT) 3000 trough modified to operate with double barriers. The surface pressure was measured with a platinum Wilhelmy plate suspended from a KSV microbalance. Infrared spectra were recorded with a Mattson Instruments (Madison, WI) Research Series-1 FTIR spectrometer with a narrow-band mercury cadmium telluride detector. LB films were deposited on OTS-covered Ge ATR crystals, and a Harrick (Ossining, NY) TMP stage was used for the ATR experiments.

Table 1. Deposition Conditions for the Preparation of Divalent Metal Octadecylphosphonate LB Films

LB film	subphase pH	target pressure (mN/m)
$Mn(O_3PC_{18}H_{37})\cdot H_2O$	5.2−5.6	20
$Cd(O_3PC_{18}H_{37})\cdot H_2O$	4.2−5.0	17
$Mg(O_3PC_{18}H_{37})\cdot H_2O$	7.4−7.6	17
$Ca(HO_3PC_{18}H_{37})_2$	7.0−8.10	17

Polarized FTIR-ATR spectra were taken with s- and p-polarized light. All ATR spectra consisted of 1000 scans at 2.0-cm^{-1} resolution and were referenced to the OTS-covered Ge ATR crystal or the appropriate s- or p-polarized background. X-ray photoelectron spectra were obtained on a Perkin-Elmer (Eden Prairie, MN) PHI 5000 series spectrometer. All spectra were taken with the Mg Kα line source at 1253.6 eV. The spectrometer had a typical resolution of 2.0 eV, with anode voltage and power settings of 15 kV and 300 W, respectively. Typical operating pressure was 5×10^{-9} atm. Survey scans were performed at a 45° take-off angle with a pass energy of 89.45 eV. Multiplex scans, 140 scans over each peak, were run over a 20−30 eV range with a pass energy of 35.75 eV. The observed relative intensities were determined from experimental peak areas normalized with atomic and instrument sensitivity factors.[35,36] X-ray diffraction was performed with a Philips APD 3720 X-ray powder diffractometer with the Cu Kα line, $\lambda = 1.54$ Å, as the X-ray source. Ellipsometry measurements were performed on a Rudolph Instruments (Fairfield, NJ) Series 431A Universal Ellipsometer with a 70° angle of incidence with a helium−neon laser, $\lambda = 632.8$ nm, as the source. Magnetization measurements were performed on a Quantum Design MPMS SQUID magnetometer. A gelcap and plastic straw were used as a sample holder during the measurements. The background signals arising from the gelcap and straw were measured independently and subtracted from the raw data.

Results

Film Deposition. The divalent metal octadecylphosphonate LB films are transferred onto solid surfaces by compressing the Langmuir monolayer to an optimum pressure, Table 1, then lowering a hydrophobic substrate through the film at 8 mm/min, transferring a monolayer in a tail-to-tail fashion on the down-stroke. The substrate is then raised from the subphase through the film at a speed of 5 mm/min, forming a head-to-head bilayer. All of the films discussed in this paper have been transferred onto solid supports that were made hydrophobic with either a self-assembled monolayer of OTS or a calcium arachidate LB film. Slow deposition speeds for the up-stroke allow draining of the water from the film and aid in the crystallization of the inorganic lattice. The metal phosphonates are soluble in acid solutions, so if the subphase pH is too low, metal ions are not incorporated into the Langmuir monolayer. If the subphase pH is too high, the Langmuir monolayer becomes too rigid to transfer as the metal ions cross-link the phosphonate groups. Therefore, the optimum subphase pH for achieving the extended lattice LB films is the highest possible pH at which the monolayer is not too rigid to transfer. This pH varied from metal to metal, and the experimentally used values are recorded in Table 1. Multilayers of the metal phosphonate films are not formed by continuous deposition because the Langmuir monolayer becomes increasingly rigid with time. Instead, one bilayer is transferred to a substrate, then the monolayer is removed from the water surface and a new octadecylphosphonic acid monolayer is formed. For each of the metal phosphonate systems studied, this deposition technique produces multilayer films with each successive transfer having a transfer ratio of 1.0 ± 0.1.

(30) Carling, S. G.; Day, P.; Visser, D.; Kremer, R. K. *J. Solid State Chem.* **1993**, *106*, 111−119.
(31) Carling, S. G.; Day, P.; Visser, D. *J. Phys.: Condens. Matter* **1995**, *7*, L109−L113.
(32) Kern, W. *J. Electrochem. Soc.* **1990**, *137*, 1887−1892.
(33) Netzer, L.; Sagiv, J. *J. Am. Chem. Soc.* **1983**, *105*, 674−676.
(34) Maoz, R.; Sagiv, J. *J. Colloid Interface Sci.* **1984**, *100*, 465−496.
(35) Wagner, C. D.; Davis, L. E.; Zeller, M. V.; Taylor, J. A.; Raymond, R. M.; Gale, L. H. *Surf. Interface Anal.* **1981**, *3*, 211.
(36) *5000 Series ESCA Systems Version 2.0 Instruction Manual*; Perkin-Elmer Physical Electronics Division: Eden Prairie, MN, 1989.

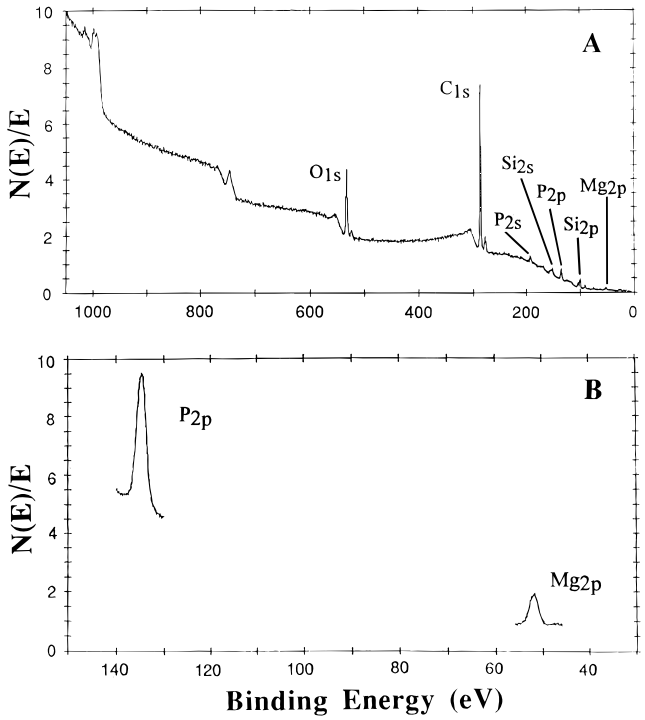

Figure 2. (A) XPS survey spectrum from one bilayer of a magnesium octadecylphosphonate LB film. (B) XPS multiplex spectrum of a single LB bilayer of magnesium octadecylphosphonate. The magnesium 2p and phosphorus 2p signals are shown. Integrated intensities are consistent with a 1:1 Mg:P ratio after accounting for the film geometry, photoelectron energies, and the appropriate elemental and instrumental sensitivity factors.

Table 2. Relative Intensities[a] of the Metal and Phosphorus XPS Signals for Single Bilayers of the Divalent Metal Octadecylphosphonate LB Films

LB film	XPS peak	obsd rel intensity (±3%)	calcd rel intensity[b] (%)
$Mn(O_3PC_{18}H_{37})\cdot H_2O$	Mn_{2p}	37	40
	P_{2p}	63	60
$Cd(O_3PC_{18}H_{37})\cdot H_2O$	Cd_{3d}	44	47
	P_{2p}	56	53
$Mg(O_3PC_{18}H_{37})\cdot H_2O$	Mg_{2p}	47	51
	P_{2p}	53	49
$Ca(HO_3PC_{18}H_{37})_2$	Ca_{2p}	29	32
	P_{2p}	71	68

[a] Intensities are reported as the percentage of the sum of the integrated areas of the metal and phosphorus peaks after correcting for elemental sensitivity factors. [b] Assuming a layered structure, using a model described in ref 37.

X-ray Photoelectron Spectroscopy. Elemental analysis of the LB films, determined by XPS, reveals that the only atoms present in the films are carbon, oxygen, phosphorus, and the appropriate metal. Figure 2 shows the XPS survey and multiplex spectra from one bilayer of a magnesium octadecylphosphonate LB film. The peak areas are integrated and corrected with atomic sensitivity factors[35,36] to yield the observed relative intensities for each element, as summarized for each of the films in Table 2. The observed intensities depend on the elemental ratios, film geometry, and photoelectron escape depths. The predicted relative XPS signal intensities were calculated for a layered film geometry using a model described previously.[37] For the Mn^{2+}, Mg^{2+}, and Cd^{2+} octadecylphosphonate LB films, the calculated ratios assume the 1:1 metal:phosphorus stoichiometry present in the $M(O_3PR)\cdot H_2O$ solid-state phases. Table 2 compares the calculated metal phosphorus ratios with the experimentally observed ratios. Within experimental uncertainty (±3%), the observed ratios for the Mn^{2+}, Mg^{2+}, and Cd^{2+} films are consistent with the bulk metal phosphonate stoichiometry.

(37) Pike, J. K.; Byrd, H.; Morrone, A. A.; Talham, D. R. *Chem. Mater.* **1994**, *6*, 1757−1765.

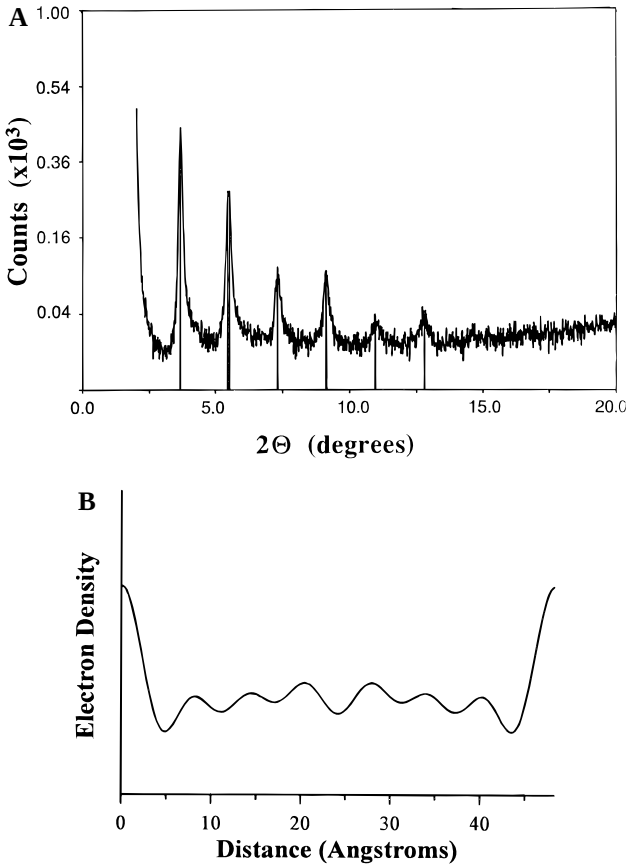

Figure 3. (A) X-ray diffraction from 15 bilayers of a cadmium octadecylphosphonate LB film. The layered nature of the film is demonstrated by the seven orders of (00*l*) reflections, corresponding to an interlayer distance of 48.2 Å. (B) Electron density profile across one unit cell of a cadmium octadecylphosphonate LB film. The region of highest electron density corresponds to those layers containing cadmium ions, and the regions of nearly uniform electron density correspond to diffraction from the alkyl chains. The region of low electron density at approximately 24 Å is a result of van der Waals interactions between the terminal methyls of the aliphatic chains.

Elemental analysis of calcium octadecylphosphonate LB films with XPS reveals a calcium-to-phosphorus ratio of 1:2. In the solid state, calcium alkylphosphonates form two layered phases with differing stoichiometries that depend on the length of the alkyl chain.[27,28] Salts with a 1:1 calcium phosphonate stoichiometry, $Ca(O_3PC_nH_{2n+1})\cdot H_2O$, form when $n = 1-5$; and 1:2 calcium phosphonates, $Ca(HO_3PC_nH_{2n+1})_2$, form for $n > 5$.[27,28] The XPS findings for the calcium phosphonate LB films are consistent with stoichiometry seen in the long-chain solid-state calcium phosphonate compounds.

Ellipsometry and X-ray Diffraction. X-ray diffraction illustrates the layered nature of the LB films. The X-ray diffraction pattern obtained from a 15-bilayer cadmium octadecylphosphonate LB film is shown in Figure 3A where several orders of 00*l* reflections are observed. Interlayer spacings derived from Figure 3A and similar diffraction patterns for the manganese, magnesium, and calcium octadecylphosphonate LB films are summarized in Table 3. Interlayer thicknesses range from 46.7 to 48.5 Å, which is reasonable for octadecylphosphonate bilayers.[20] Analysis of the Bragg intensities yields an electron density profile perpendicular to the layers in the film.

Table 3. Interlayer Spacings,[a] Indices of Refraction,[b] and Alkyl Chain Tilt Angles[c] for the Divalent Metal Octadecylphosphonate LB Films

LB film	interlayer spacing (Å) (±0.2 Å)	refractive index	tilt angle (deg)
$Mn(O_3PC_{18}H_{37})\cdot H_2O$	48.5	1.60	32
$Cd(O_3PC_{18}H_{37})\cdot H_2O$	48.2	1.55	36
$Mg(O_3PC_{18}H_{37})\cdot H_2O$	47.6	1.62	40
$Ca(HO_3PC_{18}H_{37})_2$	46.7	1.59	42

[a] Determined by X-ray diffraction from films of 15 bilayers. [b] Determined by ellipsometry. [c] Tilt angle of the alkyl chain with respect to the film normal, determined by measuring the $\nu_a(CH_2)$ band in two polarizations with ATR-FTIR.

Figure 3B shows the electron density profile across one unit cell of the cadmium octadecylphosphonate film. Following the method of Lesslauer and Blasie,[38] the electron density profile, $\rho'(x)$, was calculated by a Fourier summation with use of the Bragg intensities, $I_{obs}(h)$, from the diffraction pattern, eq 1.[38]

$$\rho'(x) = \frac{2}{D}\sum_{h=1}^{h_{max}} h\{\pm[I_{obs}(h)^{1/2}]\}\cos\left(2\pi x\frac{h}{D}\right) \qquad (1)$$

The intensities of the reflections represent the modules of the structure amplitudes, and the phases of the structure amplitudes can be either positive or negative.[39] The best profile, chosen such that the region corresponding to the aliphatic chains has nearly constant electron density, resulted from an alternation of the phase angles. In Figure 3B, the electron density maxima correspond to the metal phosphonate layers at the edges of the unit cell as expected if the metal phosphonate layers are separated by the extended alkyl chains. Similar to the electron density profiles derived for metal carboxylate films,[38] the alkyl chains give rise to a relatively constant electron density, decreasing at the terminal CH_3 groups to a minimum at the van der Waals regions between CH_3 groups. The deep minima adjacent to the maxima are due to truncation artifacts resulting from the finite number of observed Bragg reflections.[38]

The deposition of multilayered films was also followed by ellipsometry. For all of the LB films, the thickness determined by ellipsometry increases linearly with the number of layers, indicating that the same amount of material is transferred to the OTS covered silicon substrate during each deposition cycle. A plot of LB film thickness as a function of the number of layers for cadmium octadecylphosphonate is shown in Figure 4 where the solid line is a linear fit to the data. The cadmium behavior is representative of all the films. Ellipsometry relates the thickness and refractive index of a thin homogeneous film to measurable parameters, Δ and Ψ,[17] where the angles Δ and Ψ give the change in phase and change in amplitude, respectively, of plane-polarized light reflected off the film. Data obtained from ellipsometry were used in conjunction with data from the X-ray studies to calculate refractive indices of the organic films. Since interlayer distances obtained from X-ray diffraction are independent of optical constants, the value of the refractive index of the film was varied until the ellipsometric thicknesses agreed with interlayer thicknesses determined from X-ray diffraction. Refractive indices determined for the films range from 1.55 to 1.62, and the results are summarized in Table 3. Refractive indices for organic monolayers are frequently estimated to be 1.5,[40] based on the assumption that the monolayer is crystalline and its refractive index should be similar to polyethylene (1.49−1.55).[17] The introduction of metal ions should increase the refractive index of an organic film, thus substantiating the higher refractive indices observed for the metal phosphonate LB films relative to those of pure polyethylene films. The values determined for the LB films are comparable to the refractive index of 1.54 previously measured for solid-state hafnium 1,10-decanediylbis(phosphonate).[41]

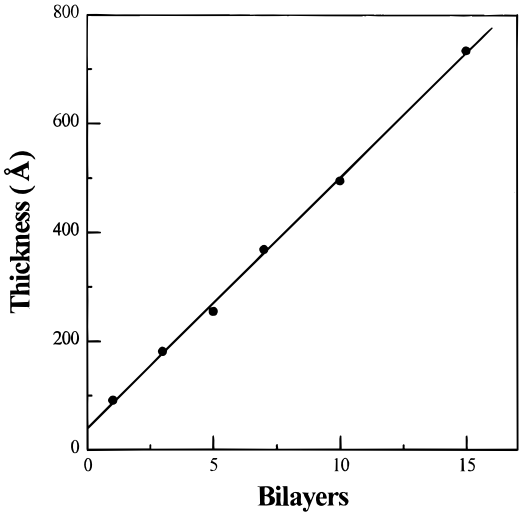

Figure 4. Ellipsometric data for a cadmium octadecylphosphonate LB film. The refractive index was varied (Table 3) to yield a best fit to the solid line with slope corresponding to the interlayer spacings obtained from X-ray diffraction. The thickness of the OTS layer and oxide layer on the silicon wafer has not been accounted for, giving rise to the non-zero thickness intercept.

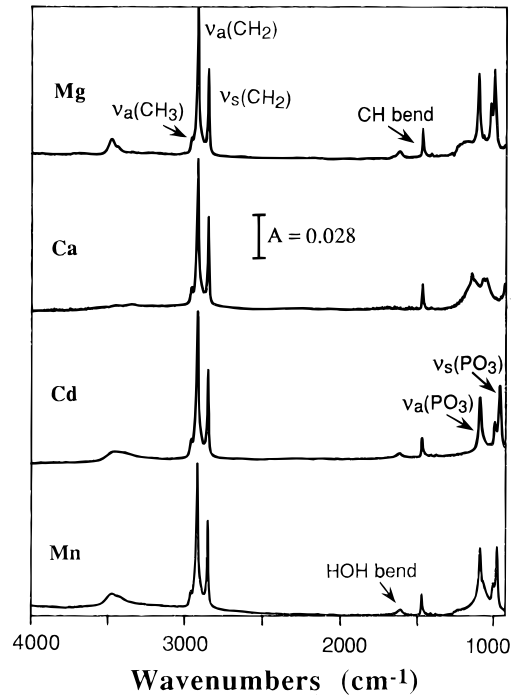

Figure 5. FTIR spectra, measured on a Ge ATR crystal, of 10-bilayer LB films of magnesium, calcium, cadmium, and manganese octadecylphosphonate. Band assignments are discussed in the text.

FTIR Spectroscopy. Figure 5 shows the FTIR spectra in the range 1000−4000 cm^{-1} of each of the divalent metal octadecylphosphonate films. Peaks at 2955, 2918, and 2850 cm^{-1} are assigned to the asymmetric methyl ($\nu_a(CH_3)$), asym-

(38) Lesslauer, W.; Blasie, J. K. *Biophys. J.* **1972**, *12*, 175.
(39) Nicolini, C. *Molecular Bioelectronics*; World Scientific: Singapore, 1990.
(40) Allara, D. L.; Nuzzo, R. G. *Langmuir* **1985**, *1*, 45.
(41) Zeppenfeld, A. C.; Fiddler, S. L.; Ham, W. K.; Klopfenstein, B. J.; Page, C. J. *J. Am. Chem. Soc.* **1994**, *116*, 9158−9165.

metric methylene ($\nu_a(CH_2)$), and symmetric methylene ($\nu_s(CH_2)$) stretches, respectively, of the octadecyl chain. It has been shown that the position and shape of the $\nu_a(CH_2)$ and $\nu_s(CH_2)$ absorption bands reflect the conformational order and packing of the aliphatic chains in monolayers.[34,42,43] For long-chain hydrocarbons, such as *n*-alkanethiols or polyethylene, the energy of the $\nu_a(CH_2)$ band ranges from 2918−2920 cm^{-1} (when the aliphatic chain is in an all-trans conformation) to 2924−2928 cm^{-1} (when a "liquid-like" alkane contains a large percentage of gauche bonds).[34,42] The observed position of the $\nu_a(CH_2)$ IR band at 2918 cm^{-1} in each divalent metal octadecylphosphonate LB film implies the alkyl chains are fully extended with all-trans conformation. The $\nu_s(CH_2)$ band is also an indicator of the state of the hydrocarbon chains. This band is particularly sensitive to the average local environment of an individual chain within the monolayer, indicating the density of packing of the monolayer.[42,43] The peak position of the $\nu_s(CH_2)$ band for crystalline hydrocarbons lies at 2850 cm^{-1} and shifts to higher energies, 2856 cm^{-1}, as the hydrocarbon chains become less close packed.[42] The appearance of the $\nu_s(CH_2)$ band at 2850 cm^{-1} for each ocadecylphosphonate LB system is consistent with high-density, crystalline-like phases in the LB films. The full width at half maximum, fwhm, of the $\nu_a(CH_2)$ absorption band is another measure of the conformational order of the alkyl chains in the films,[34,42] where an organized close-packed monolayer gives a fwhm of 17 cm^{-1} and a randomly oriented film can result in a fwhm of greater than 35 cm^{-1}.[20,44] A fwhm of 17 cm^{-1} of the $\nu_a(CH_2)$ bands in each of the divalent metal phosphonate LB films is consistent with the peak-position analyses and indicates crystal-like organization of the all-trans alkyl chains. The position and shape of these hydrocarbon stretching modes do not change with the deposition of additional bilayers, indicating that the films maintain their structure with each successive transfer.

The appearance of two unresolved bands at approximately 3400 cm^{-1} and a band at 1608 cm^{-1} in the IR spectra of all but the calcium octadecylphosphonate LB films indicates the presence of lattice water in the LB films. Lattice water absorbs at 3550−3200 and at 1630−1600 cm^{-1} due to OH stretching modes and HOH bending modes, respectively.[45] In bulk manganese, cadmium, and magnesium alkylphosphonates, each metal ion is bound by five oxygen atoms from the phosphonate anions and oxygen from water fills the sixth coordination site.[27−29] For the LB films formed with these metal ions, the intensity of the water bending mode was followed as successive bilayers were transferred to a Ge ATR crystal, Figure 6. A linear increase in area of the water bending mode with increasing number of layers suggests that the water is stoichiometrically incorporated into the lattice and is consistent with coordination of water to the metal ions. In addition, the relative intensities of the water bending modes versus the PO_3^{2-} stretching modes in the LB films are similar to the relative intensities seen in the powdered solids (for example, Figure 7). This further suggests that the coordinated water is included in the metal−phosphonate lattice of the LB film, as it is in the analogous solid-state metal phosphonates.

The absence of the water modes in the calcium film is further evidence that the calcium octadecylphosphonate LB film forms the same structure as the 1:2 calcium:phosphorus solid-state phase. The main differences in the structure between solid-state calcium organophosphonates with a 1:1 calcium:phosphorus stoichiometry and those with a 1:2 ratio lie in the coordination environment of the calcium ion. Calcium ions in the 1:1 salts have an approximately pentagonal-bipyramidal coordination bound by 7 oxygens, one of which is a water of hydration.[28] In the 1:2 calcium salts, calcium atoms are bound by six oxygens from RPO_3H^- groups, resulting in a distorted octahedral environment. In these compounds, the hydroxyl group of the RPO_3H^- ion is not coordinated to calcium, and no water is bound to the calcium ions.[28] The absence of the water ν(OH) and HOH bend absorptions in the LB film of calcium octadecylphosphonate suggests that the film structure is more like that of the 1:2 salt.

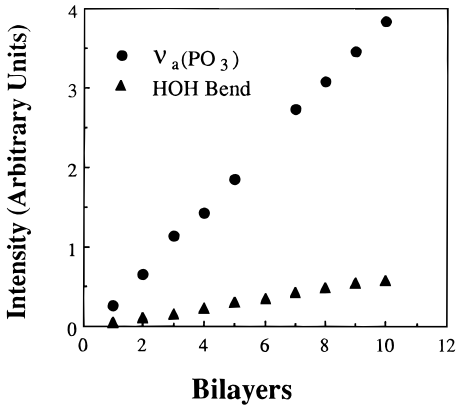

Figure 6. Integrated intensity of the $\nu_a(PO_3^{2-})$ and HOH bend FTIR absorptions as a function of the number of bilayers for a manganese octadecylphosphonate LB film. The linear increase in the FTIR band intensities is evidence that the composition of the film is maintained throughout the deposition process. A linear increase in the intensity of the water bending mode is evidence for the stoichiometric incorporation of H_2O into the LB film.

To make additional structural comparisons, the IR spectra of the phosphonate LB films were compared to the IR spectra of solid-state metal alkylphosphonates. To illustrate, the 900−1800-cm^{-1} region of the infrared spectra for both a powder sample of cadmium ethylphosphonate and the cadmium octadecylphosphonate LB film are compared in Figure 7. Progressions of peaks in the 1175−1400-cm^{-1} region are assigned to CH_2 rocking and wagging modes of all-trans alkyl chains[46] in both the LB films and the powdered solids. Also common to both solid-state alkylphosphonates and the analogous LB films are small methylene scissor deformation bands, observed at 1467 and 1410 cm^{-1} in the LB films. The latter band corresponds to the CH_2 group adjacent to the phosphonate group.[47,48] The absence of a strong P═O stretch[47,49] in the 1350−1250-cm^{-1} region or the 1250−1110-cm^{-1} region for free and hydrogen bonded modes, respectively, indicates that all of the phosphonate groups are ionized in the LB film as they are in the solid-state sample. On the other hand, the PO_3^{2-} stretching modes are strong and well-resolved in both the LB films and powdered solids. In the LB film spectrum in Figure 7, the band at 1089 cm^{-1} is assigned to the asymmetric PO_3^{2-} stretch and bands at 992 and 960 cm^{-1} are the symmetric PO_3^{2-} stretches, split as a result of the lower than C_{3v} local symmetry of the phosphonate groups. The analogous bands appear at 1089, 984, and 957 cm^{-1} in the cadmium ethylphosphonate powder. The PO_3^{2-}

(42) Porter, M. D.; Bright, T. B.; Allara, D. L.; Chidsey, C. E. D. *J. Am. Chem. Soc.* **1987**, *109*, 3559−3568.
(43) Wood, K. A.; Snyder, R. G.; Strauss, H. L. *J. Chem. Phys.* **1989**, *91*, 5255−5267.
(44) Byrd, H.; Whipps, S.; Pike, J. K.; Talham, D. R. *Thin Solid Films* **1994**, *244*, 768−771.
(45) Nakamoto, K. *Infrared and Raman Spectra of Inorganic and Coordination Compounds*, 3rd ed.; John Wiley & Sons: New York, 1978.
(46) Susi, H.; Smith, A. M. *J. Am. Oil Chem. Soc.* **1960**, *37*, 431−435.
(47) Bellamy, L. J. *The Infra-red Spectra of Complex Molecules*, 3rd ed.; Chapman and Hall: London, 1975.
(48) Hayaki, J. *J. Chem. Phys.* **1975**, *63*, 1732.
(49) Thomas, L. C.; Chittenden, R. A. *Spectrochim. Acta* **1970**, *26A*, 781−800.

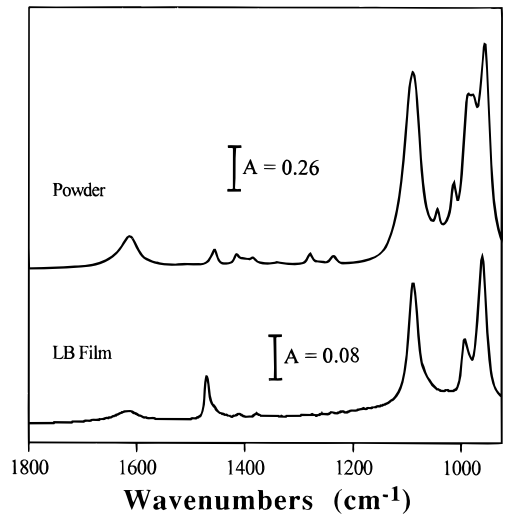

Figure 7. FTIR comparison of (A) a KBR pellet of powdered cadmium ethylphosphonate and (B) three bilayers of a cadmium octadecylphosphonate LB film deposited onto a germanium ATR crystal. The positions of the phosphonate stretching bands in the two materials are an indicator of the structural similarities. Band assignments are discussed in the text.

Table 4. Comparison of the Infrared $\nu(PO_3^{2-})$ Frequencies of Divalent Metal Alkylphosphonate Powders and LB Films

compd	$\nu_a(PO_3^{2-})$ (cm^{-1})	$\nu_s(PO_3^{2-})$ (cm^{-1})
$Mn(O_3PC_2H_5)\cdot H_2O$[a]	1087	1017, 988, 964
$Mn(O_3PC_{18}H_{37})\cdot H_2O$[b]	1087	1003, 977
$Cd(O_3PC_2H_5)\cdot H_2O$[a]	1089	984, 957
$Cd(O_3PC_{18}H_{37})\cdot H_2O$[b]	1089	992, 960
$Mg(O_3PC_{18}H_{37})\cdot H_2O$[b]	1102	1024, 999
$Ca(O_3PC_2H_5)\cdot H_2O$[a]	1093	1026, 993
$Ca(HO_3PC_{10}H_{21})_2$[a]	1146	1072, 1045
$Ca(HO_3PC_{18}H_{37})_2$[b]	1146	1072, 1045

[a] Powder sample, measured as KBr pellet. [b] LB film, measured on the Ge ATR crystal.

stretching modes are very sensitive to local symmetry,[28,50] and the close agreement between the frequencies observed for the LB film and those seen for the powdered solids indicates that the LB films have the same phosphorus−oxygen−metal−water extended lattice network as the solid compounds. The frequencies of the PO_3^{2-} stretching modes for each of the LB films are listed in Table 4 along with the frequencies observed in analogous solid-state samples. Like the cadmium case, the phosphonate binding in the manganese and magnesium phosphonate films is similar to the corresponding solid-state $M(O_3PR)\cdot H_2O$ phase. The IR spectrum of the calcium octadecylphosphonate LB film is compared to those of calcium decylphosphonate and calcium ethylphosphonate in Figure 8. There are differences in the P−O stretching region of the two solid-state calcium phosphonate compounds arising from the different structures of the two phases. The P−O stretching region of the calcium phosphonate LB film is remarkably similar to that of calcium decylphosphonate. This result, in agreement with XPS data, illustrates that the structure of the calcium octadecylphosphonate film fabricated with LB methods is similar to the calcium alkylphosphonate solid-state compounds of molecular formula $Ca(HO_3PC_nH_{2n+1})_2$.

Polarized ATR-FTIR was used to establish the tilt angles of the octadecylphosphonate molecules in the divalent metal phosphonate LB films. The tilt angle of IR-active vibrational modes within layered organic films can be determined from

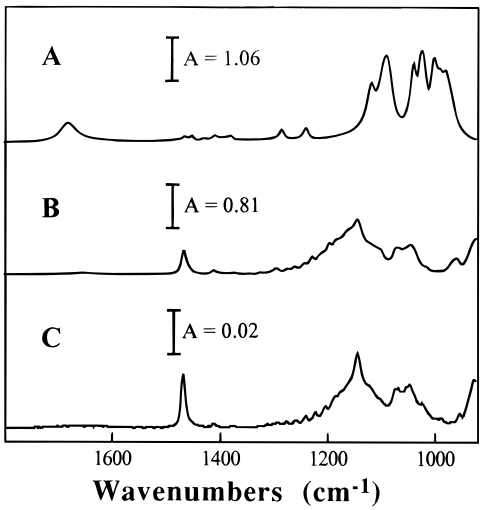

Figure 8. FTIR spectra of (A) a KBr pellet of calcium ethylphosphonate, $Ca(O_3PC_2H_5)\cdot H_2O$, (B) a KBr pellet of calcium decylphosphonate, $Ca(HO_3PC_{10}H_{21})_2$, and (C), and an LB film of calcium octadecylphosphonate on a Ge ATR crystal. The similarity of the spectra of the solid-state calcium decylphosphonate and the calcium octadecylphosphonate LB film suggests the LB film structure is comparable to the structure of those solid-state calcium alkylphosphonates containing long-chain alkyl groups.

the ratio of IR absorbances measured in two polarization directions.[17,51,52] The absorbance of the $\nu_a(CH_2)$ band was recorded with s- and p-polarized light for each film, and the resulting tilts of the alkyl chain with respect to the normal of the metal ion plane are given in Table 3. Since the LB films are each comprised of octadecylphosphonate bilayers, their layer thickness should be similar, with differences arising from variations in the tilting of the alkyl chains. The less the alkyl chains tilt from the normal, the larger the layer thickness. The alkyl chain tilt angles, determined by polarized FTIR, are similar for each of the films and are consistent with the layer thicknesses measured by X-ray diffraction.

A Magnetic Langmuir−Blodgett Film. The magnetic properties of a series of solid-state manganese alkylphosphonates $Mn(O_3PC_nH_{2n+1})\cdot H_2O$, $n = 1-4$, were investigated by Carling *et al.*,[30,31] and these authors showed that at high temperatures the manganese phosphonates can each be characterized as a 2-dimensional lattice of $S = {}^5/_2$ Mn^{2+} ions with Heisenberg antiferromagnetic nearest-neighbor exchange. At lower temperatures (14.8−15.1 K), each member of the series undergoes a magnetic ordering transition where the ordered state has a weak spontaneous magnetization due to incomplete cancellation of the antiferromagnetically coupled moments. Such systems are known as canted antiferromagnets or "weak ferromagnets". We previously reported observation of antiferromagnetic exchange in an EPR study of the manganese octadecylphosphonate LB film, confirming that the in-plane structure of the film is analogous to the solid-state layered solids.[22] The 9.3-GHz EPR line width ranges from 218 to 300 G depending on the orientation of the film in the magnetic field, and the angular dependence of the line width is consistent with magnetic exchange in a two-dimensional lattice.[22] The temperature dependence of the EPR intensity was used to estimate the magnitude of the nearest-neighbor exchange, *J*, by fitting the

(50) Frey, B. L.; Hanken, D. G.; Corn, R. M. *Langmuir* **1993**, *9*, 1815−1820.

(51) Haller, G. L.; Rice, R. W. *J. Phys. Chem.* **1970**, *74*, 4386−4393.

(52) Tillman, N.; Ulman, A.; Schildkraut, J. S.; Penner, T. L. *J. Am. Chem. Soc.* **1988**, *110*, 6136−6144.

(53) Navarro, R. In *Magnetic Properties of Layered Transition Metal Compounds*; de Jongh, L. J., Ed.; Kluwer Academic Publishers: Dordrecht, 1990; pp 105−190.

(54) Rushbrooke, G. S.; Wood, P. J. *Mol. Phys.* **1958**, *1*, 257.

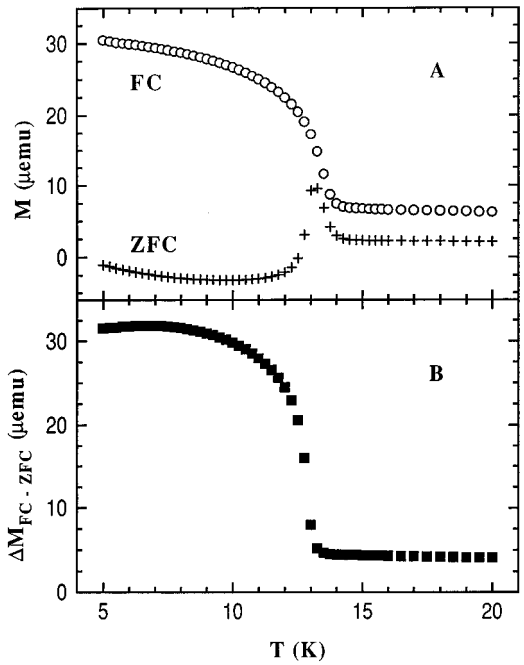

Figure 9. Magnetization *vs* temperature for an 81-bilayer film of manganese octadecylphosphonate with the measuring field applied parallel to the plane of the film. (A) Comparison of the data taken upon warming the film after cooling in zero applied field (ZFC) and cooling in a field of 0.1 T (FC). In both cases the measuring field is 0.01 T. The ordering transition (T_N) is seen as the discontinuity in the ZFC plot at 13.5 K. (B) The difference of the two plots in part A showing the spontaneous magnetization below T_N.

intensity data to a numerical expression[53,54] for the susceptibility of a quadratic layer Heisenberg antiferromagnet. A value of $J/k_B = -2.8$ K was obtained[22] from the fit, which is nearly identical with the values of $J/k_B = -2.70$ and -2.78 K found by Carling et al.[30,31] for the solid-state manganese methylphosphonate and manganese ethylphosphonate, respectively. However, a transition to long-range magnetic order is not seen in the EPR. In both the LB film and the powdered solid-state analogs, the line width begins to increase below 50 K and becomes too broad to measure below 17 K. This behavior is consistent with antiferromagnetic fluctuations, a precursor to magnetic ordering, but no direct observation of the ordered state can be seen in the EPR at 9.3 GHz. After magnetic order is established, the internal fields shift the electronic resonances (antiferromagnetic resonance) outside the frequency-field space probed by X-band.[55]

However, an ordering transition is observed in static magnetization measurements. The temperature dependence of the magnetic susceptibility was measured with a commercial SQUID magnetometer. Two independent samples were measured, one with 50 bilayers and one with 81 bilayers, and each exhibited the same magnetic behavior. For the magnetic measurements, samples were deposited onto both sides of a mylar sheet, which was then cut up into small pieces (3 mm × 3 mm). The mylar pieces were stacked and oriented in a gelcap that was held in the magnetometer with a plastic straw. The background contribution of the gelcap and straw was measured independently and subtracted from the data. Data for the 81-bilayer film (total area of 5.5 cm^2 giving a sample of 6×10^{-7} mol) are presented in Figure 9. The temperature-dependent magnetization, measured upon warming the film between 5 and 25 K and recorded with the measuring field of 0.01 T parallel to the plane of the film, is shown in Figure 9A for the cases where the sample was cooled from room temperature in zero applied field (ZFC) and where the sample was cooled from room temperature in a magnetic field of 0.1 T (FC). The ZFC data show the signature of an ordering transition at 13.5 K. The FC data also show the ordering transition, and the increased magnetization below the ordering temperature (T_N) is evidence for spontaneous magnetization of the film. The spontaneous magnetization is shown more clearly in Figure 9B, where the difference between the FC and ZFC magnetization (ΔM) is plotted. While the mass of the sample is small compared to that of the sample holder and mylar substrate, the difference plot subtracts the signal due to the sample support and allows quantification of the film magnetization. Below T_N, the magnetization increases and begins to level off as the temperature approaches 5 K. The magnitude of the magnetization is small, and the moment at 5 K corresponds to a ferromagnetic moment of $\mu_{ferro}/\mu_B = 8 \times 10^{-3}$. The weak moment in the ordered state is consistent with antiferromagnetic ordering of the lattice where coupled nearest neighbor moments do not exactly cancel, due to low site symmetry, giving rise to a "weak ferromagnetic" state. The magnitude of the ferromagnetic moment is similar to the moments observed for the manganese alkylphosphonate solid-state analogs.[30]

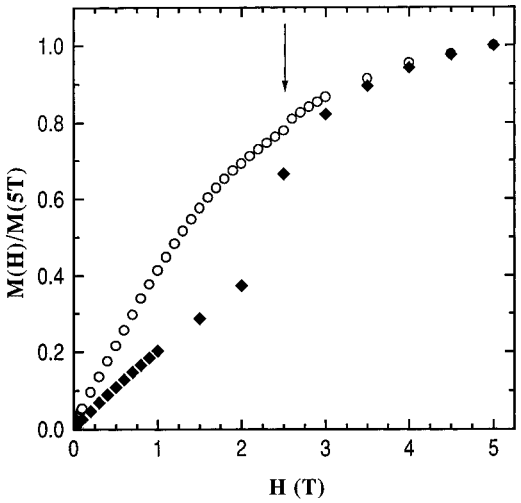

Figure 10. Magnetization *vs* applied field at 2 K, normalized to the value at 5 T, with the applied field directed perpendicular (filled diamonds) and parallel (open circles) to the plane of the sample. The spin-flop transition is seen in the perpendicular orientation at 2.5 T (the easy axis is perpendicular to the sample plane). A small inflection at 2.5 T is also seen in the parallel orientation due to imperfect alignment of the individual mylar sheets with respect to the field.

Field-dependent magnetization measured at 2 K at applied fields up to 5 T is shown in Figure 10 for two orientations of the film. For the case where the applied field is oriented perpendicular to the plane of the film, there is evidence for a spin-flop transition at $H_{app} = 2.5$ T. The spin-flop transition in this orientation indicates that the axis of antiferromagnetic alignment is perpendicular to the plane of the film and therefore perpendicular to the manganese phosphonate layers. While the magnetic structures of the solid-state organophosphonates have not yet been determined, the magnetic structure of a purely inorganic isomorph, $KMnPO_4 \cdot H_2O$, has been determined from magnetic scattering in its neutron diffraction profile.[56] The structure shows that the manganese moments are antiferromagnetically coupled within the manganese phosphate planes and

(55) Katsumata, K.; Tuchendler, J. *J. Phys. C: Solid State Phys.* **1987**, *20*, 4873−4879.

(56) (a) Visser, D.; Carling, S. G.; Day, P.; Deportes, J. *J. Appl. Phys.* **1991**, *69*, 6016−6018. (b) Carling, S. G.; Day, P.; Visser, D. *Inorg. Chem.* **1995**, *34*, 3917−3927.

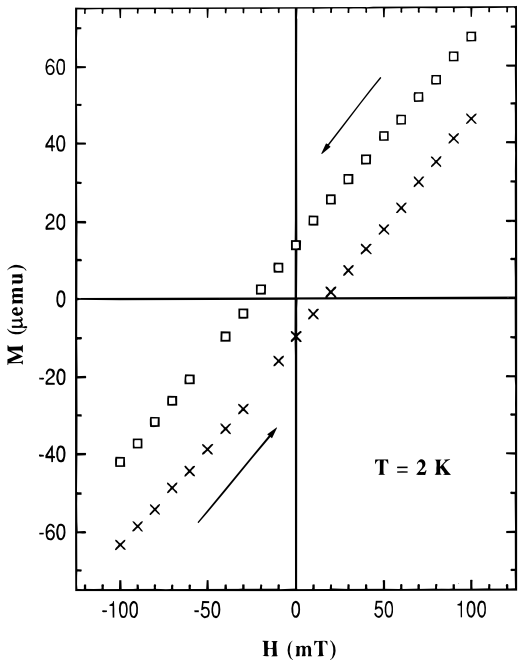

Figure 11. Magnetization at 2 K in the viscinity of zero field showing hysteresis during cycling between +5 and −5 T. The applied field is oriented perpendicular to the plane of the film. A remnant magnetization of 10 μemu and a coercive field of 20 mT are observed.

aligned perpendicular to the planes, which is consistent with the behavior observed for the LB film. Canting of the antiferromagnetically coupled moments therefore puts the "weak ferromagnetic" moment in the manganese phosphonate plane, or parallel to the plane of the film. This behavior is also observed in $KMnPO_4 \cdot H_2O$, where the canting is in-plane toward the crystallographic *c*-axis.[56] With the field oriented parallel to the plane of the LB film, the magnetization gradually increases with increasing applied field (Figure 10) as is expected if the antiferromagnetic hard axis lies in the plane. There is a small inflection corresponding to the spin-flop transition seen at $H_{app} = 2.5$ T that is attributed to imperfect alignment of the sample with respect to the external field.

The LB film also exhibits magnetic memory below T_N. Figure 11 plots magnetization in the vicinity of zero field for positive and negative scans of the applied field as the magnetic field is cycled between +5 and −5 T. Hysteresis is the signature of magnetic memory, and a small coercive field of 20 mT and remnant magnetization of 10 μemu are seen. Although the effect is small, the result nevertheless demonstrates that the LB method can be used to produce thin magnetic films.

Discussion

As far as we are aware, the canted antiferromagnetic state of manganese octadecylphosphonate is the first example of magnetic order in an LB film. Magnetic studies of LB films are mostly limited to EPR determination of the orientation of organic radicals or metal complexes in transferred films. While evidence for magnetic exchange between molecular species in LB films has been observed in some instances,[57−60] there are no examples of magnetically ordered molecular films. The most extensive investigations of magnetism in LB films have focused on manganese stearate.[61−64] In the pioneering work of Pomerantz,[61−64] antiferromagnetic exchange was observed by EPR and precursor effects to antiferromagnetic ordering were seen in the EPR line width and *g*-value at temperatures approaching 2 K. However, an ordering transition has not been observed, and there have been no measurements of the ordered state. The enhanced magnetic exchange in the manganese phosphonate films, relative to the manganese stearate films, is due to superexchange *via* the phosphonate ligand (Figure 1). The solid-state inorganic lattice provides sufficient structural order for magnetic ordering to take place.

We can comment on the nature of the magnetic order and what it indicates about the composition of the LB layers. Magnetic exchange in a 2-dimensional lattice can be described by eq 2 where S_i and S_{i+1} are nearest-neighbor spins.

$$H = -2J\sum_i \{\alpha S_{iz}S_{(i+1)z} + \beta(S_{ix}S_{(i+1)x} + S_{iy}S_{(i+1)y})\} \quad (2)$$

Normally, for a Mn^{2+} ion with $S = {}^5/_2$, $\alpha = \beta = 1$, which is called the Heisenberg limit.[64] At high temperature ($T > T_N$) the magnetic susceptibility in both the manganese octadecylphosphonate LB film and the powdered manganese phosphonates[30] is well described with a model for 2-dimensional Heisenberg exchange. It has been well understood for some time that a truly 2-dimensional Heisenberg lattice cannot undergo a transition to long-range magnetic order.[65] For a 2-dimensional Heisenberg system to order, there must be some interlayer magnetic exchange, J', that leads to a 3-dimensional ordered state. Ordering in 2-dimensions can occur, however, if there is some anisotropy in the in-plane magnetic exchange ($\alpha \neq \beta$ in eq 2) or if there is sufficient single ion anisotropy (the local manganese ion symmetry is lower than O_h).[66] In most layered 2-dimensional model systems that have been studied, ordering is observed and there is a competition between 3-dimensional ordering and 2-dimensional ordering.[67] In fact, there is often a crossover from 2-dimensional behavior to 3-dimensional behavior below T_N. The driving force for 3-dimensional order is J', while for systems with very small interlayer interaction, 2-dimensional order is driven by the divergence of the magnetic correlation length, ξ, as the temperature is lowered toward T_N.[67] The compound K_2MnF_4 provides an example of a layered manganese compound where the in-plane correlation length exceeds the interlayer coupling and 2-dimensional ordering is observed.[67,68] For a related series of layered antiferromagnets, $[NH_3(CH_2)_3NH_3]MnCl_4$, $(CH_3NH_3)_2MnCl_4$, and $(XC_6H_4NH_3)_2MnCl_4$ (X = F, Cl, Br, or *n*-Bu), Hatfield et al. showed that the temperature at which long-range order occurs decreases slightly with increasing interlayer separations, but becomes practically independent when the spacing exceeds about 15 Å.[69] In these systems, it is thought that anisotropy in the 2-dimensional Hamiltonian (eq 2) is the driving

(57) Bonosi, F.; Gabrielli, G.; Martini, G.; Ottaviani, M. F. *Langmuir* **1989**, *5*, 1037−1043.
(58) Ikegami, K.; Kuroda, S.-I.; Sugi, M.; Nakamura, T.; Tachibana, H.; Matsumoto, M.; Kawabata, Y. *J. Phys. Soc. Jpn.* **1992**, *61*, 3752−3765.
(59) Ikegami, K.; Kuroda, S.-I.; Sugi, M.; Tachibana, H.; Nakamura, T.; Matsumoto, M. *Thin Solid Films* **1994**, *242*, 11−15.
(60) Suga, K.; Iwamoto, Y.; Fujihira, M. *Thin Solid Films* **1994**, *243*, 634−637.
(61) Pomerantz, M. *Surf. Sci.* **1984**, *142*, 556−570.
(62) Pomerantz, M. *Solid State Commun.* **1978**, *27*, 1413−1416.
(63) Pomerantz, M.; Dacol, F. H.; Segmüller, A. *Phys. Rev. Lett.* **1978**, *40*, 246−249.
(64) Ferrieu, F.; Pomerantz, M. *Solid State Commun.* **1981**, *39*, 707−710.
(65) Mermin, N. D.; Wagner, H. *Phys. Rev. Lett.* **1966**, *17*, 1133−1136.
(66) Onsager, L. *Phys. Rev.* **1944**, *65*, 117−149.
(67) de Jongh, L. J. In *Magnetic Properties of Layered Transition Metal Compounds*; de Jongh, L. J., Ed.; Kluwer Academic Publishers: Dordrecht, 1990; pp 1−51.
(68) Benner, H.; Boucher, J. P. In *Magnetic Properties of Layered Transition Metal Compounds*; de Jongh, L. J., Ed.; Kluwer Academic: Dordrecht, 1990; pp 323−378.
(69) Blake, A. B.; Hatfield, W. E. *J. Chem. Soc., Dalton Trans.* **1979**, *11*, 1725−1729.

force for the ordering transition rather than the interlayer exchange.[67,70]

In the manganese octadecylphosphonate LB film where the separation between magnetic planes is very large, 50 Å, it is unlikely that onset of the ordered state is due to interlayer exchange. Rather, in analogy to other Mn^{2+} layered compounds, the magnetic correlation length within the manganese layers must be large and responsible for the ordered state. The magnetic correlation length in the LB film can be estimated by using predictive models that have previously been shown to accurately reproduce the correlatation lengths determined experimentally by neutron scattering in layered solids at temperatures above T_N.[71,72] Using the approach of Elstner et al.[72] for an $S = {}^5/_2$ square lattice Heisenberg antiferromagnet and taking $-J/k_B = 2.8$ K, an in-plane correlation length of $35a$ is calculated at 14 K, just above the ordering temperature, where a is the in-plane lattice constant. Assuming $a \approx 5$ Å, near the value seen in the solid-state manganese phosphonates, ξ is estimated to be 175 Å at 14 K. As T_N is approached from the high-temperature side ξ has an exponential dependence that diverges at T_N, and 175 Å can be regarded as a lower limit of ξ in the ordered state since it is estimated above T_N in the non-ordered state.

Since the magnetic correlation length within the manganese planes can be no larger than the structural correlation length, 175 Å can also be regarded as a lower limit estimate of the size of structurally ordered domains. Preliminary AFM analyses confirm the presence of domains of at least this size.[73] Low-resolution AFM profiles (Supporting Information) show the films are smooth, and consist of well-defined domains, typically with diameters ranging from 200 to 700 Å. Low-resolution AFM cannot determine if there is crystalline order within the domains, but their presence is consistent with the correlation lengths estimated from the magnetic properties. Studies of dilute layered antiferromagnets have shown that the addition of impurities to physically limit ξ greatly reduces T_N or even completely suppresses ordering.[71] We have shown this to be the case with the manganese phosphonate LB film. By purposely incorporating nonmagnetic Cd^{2+} ions into the manganese phosphonate lattice, magnetic ordering can be pushed to lower temperature or completely eliminated. As little as 12% Cd^{2+} doping completely suppresses ordering. This observation is consistent with what is know about 2-dimensional antiferomagnetic ordering[67] and adds further evidence that the LB film is behaving as a layered 2-dimensional solid. Based on what is known about magnetic ordering in layered systems, it can be concluded that at and below T_N, the LB film is comprised of magnetically and structurally ordered domains of at least 10^4-10^5 Å^2 in size. It is worth emphasizing that the situation described here for 2-dimensional ordering in layered materials is fundamentally different from 3-dimensional ordering or the magnetism seen in ultrasmall or nanoscale magnetic particles. In those materials where exchange pathways are present in three dimensions, long-range ordering can result from smaller correlation lengths or much smaller single domains. Larger correlation lengths are required for 2-dimensional order because J' is absent.

When comparing the structural characterization of the different LB films and taking into account the magnetic properties of the manganese phosphonate film, it can be concluded that each divalent metal phosphonate LB film forms with a solid-state ionic−covalent metal phosphonate network. The metal phosphonate bonding in each case is understood by comparing the LB films to known metal phosphonate solids, and each film adopts a known solid-state layered structure. The in-plane layered structure is determined by optimizing the metal−phosphonate binding. Although the organic groups are the same in each case, even the metal-to-phosphonate ratios can be changed by choice of divalent metal. This is dramatically illustrated by the different structures seen for the Cd^{2+} and Ca^{2+} films where the ionic radii are expected to be similar.[28,29] Such differences are well-known in solid-state chemistry, but are not as widely considered when evaluating LB film structure, although the importance of the metal/headgroup interaction has recently been pointed out in structural studies of a series of metal carboxylate LB films.[19]

The analyses suggest that the films are nearly exclusively composed of crystalline domains with a high degree of local order. XPS data indicate that the $M(O_3PR)\cdot H_2O$ films are all fully ionized. In the FTIR, the PO_3^{2-} stretching modes are very sensitive to the mode of phosphonate binding,[28,50] and in the LB films they are as well resolved as they are in the solids, indicating that the metal phosphonate binding is uniform throughout the film. There is no evidence for large areas of amorphous metal−phosphonate structure. Perhaps the most compelling indication that the in-plane order is uniform comes from the magnetic studies on the manganese phosphonate film. Below the magnetic ordering temperature there is no sign of residual paramagnetic sites giving rise to a Curie tail in the ZFC SQUID measurement, nor is there an additional signal in the EPR.[22] Isolated manganese ions that might be expected if there was a high density of disordered regions in the film would be visible as paramagnetic impurities. Within the sensitivities of the two magnetic techniques, all of the manganese ions in the film are part of highly ordered manganese phosphonate domains.

The metal phosphonate structures are formed during the deposition process. The metal phosphonate "precipitates" upon draining of water from the film as the substrate is withdrawn from the subphase. Since the source of organophosphonic acid is restricted to the pre-arranged Langmuir monolayers, the metal phosphonate "crystallization" is controlled by the deposition procedure. The deposition is limited to a single layer at a time, and the metal phosphonate layers grow exclusively parallel to the substrate. We have thus far chosen to minimize the substrate's influence on the LB film by depositing onto surfaces made hydrophobic with OTS or calcium arachidate, thereby allowing the metal/phosphonate binding to dictate the in-plane structure of each bilayer. The in-plane orientation might ultimately be controlled if an appropriate substrate were identified that could impose a preferred orientation on the depositing film.[19,74]

Conclusion

Structural characterization shows that octadecylphosphonate LB bilayers with divalent metals appear to be isostructural with their solid-state metal phosphonate analogs, demonstrating that Langmuir−Blodgett methods can be used to form monolayer and multilayer films of known solid-state materials. The structures are deposited one layer at a time, and the LB film method represents a wet-chemical way of depositing single

(70) Hatfield, W. E.; Estes, W. E.; Marsh, W. E.; Pickens, M. W.; ter Haar, L. W.; Weller, R. R. In *Extended Linear Chain Compounds*; Miller, J. S., Ed.; Plenum Press: New York, 1983; Vol. 3, pp 43−142.

(71) Endoh, Y.; Yamada, K.; Birgeneau, R. J.; Gabbe, D. R.; Jenssen, H. P.; Kastner, M. A.; Peters, C. J.; Picone, P. J.; Thurston, T. R.; Tranquada, J. M.; Shirane, G.; Hidaka, Y.; Oda, M.; Enomoto, Y.; Suzuki, M.; Murakami, T. *Phys. Rev. B* **1988**, *37*, 7443−7453.

(72) Elstner, N.; Sokol, A.; Singh, R. R. P.; Greven, M.; Birgeneau, R. J. *Phys. Rev. Lett.* **1995**, *75*, 938−941.

(73) Seip, C. T.; Ravaine, S.; Talham, D. R. Unpublished results.

(74) Schwartz, D. K.; Viswanathan, R.; Garnaes, J.; Zasadzinski, J. A. *J. Am. Chem. Soc.* **1993**, *115*, 7374−7380.

layers of ionic−covalent inorganic solids. Normally, thin films of inorganic solids are fabricated with use of vacuum deposition techniques. The structure of each octadecylphosphonate LB film depends on the identity of the metal ion, just as do the solid-state materials. It is the metal/phosphonate binding interaction that determines the film structure.

The observation of magnetic order in the manganese octadecylphosphonate LB film is further evidence that the LB films have the same in-plane structure as the layered solids. The spontaneous magnetization demonstrates that important physical phenomena can be introduced via the inorganic network in mixed organic/inorganic LB films. The possibility now exists of developing LB films where the organic layer also has function, resulting in organic/inorganic assemblies in which the inorganic and organic networks complement each other, leading to potentially new properties.

Acknowledgment. This work was supported by the National Science Foundation, in part by DMR-9200671 (M.W.M.) and DMR-9530453 (D.R.T.). We thank Prof. J. R. Childress for making the magnetometer available to us (acquired through an NSF instrumentation grant, DMR-9422192). We thank the University of Florida Major Analytical Instrumentation Center for instrument time. We are grateful to Andy Boeckl for assisting with the X-ray diffraction measurements, Dr. Serge Ravaine for AFM images, and Prof. Houston Byrd for helpful discussions.

Supporting Information Available: AFM image from one bilayer of a manganese octadecylphosphonate LB film on an OTS covered silicon substrate (1 page). See any current masthead for ordering and Internet access instructions.

JA963598C